

# Transurethral Multi-Sectored Ultrasound Applicators for Conformal Thermal Therapy of the Prostate with MR Temperature Monitoring

A. M. Kinsey<sup>1,2</sup>, C. J. Diederich<sup>1,2</sup>, W. H. Nau<sup>1</sup>, K. Butts Pauly<sup>3</sup>, V. Rieke<sup>3</sup>, G. Sommer<sup>3</sup>

<sup>1</sup>Thermal Therapy Research Group, Radiation Oncology, University of California, San Francisco, San Francisco, CA, United States, <sup>2</sup>Joint Graduate Group in Bioengineering, University of California, Berkeley and San Francisco, San Francisco, CA, United States, <sup>3</sup>Radiology, Stanford University, Stanford, CA, United States

**Introduction** High-temperature thermal therapy (>50 °C, lethal thermal dose) of cancer and benign disease in the prostate has been investigated extensively as an alternative to surgery and as a complement to other treatment modalities. The accuracy and long duration of delivering treatment remains an obstacle to widespread clinical acceptance of thermal therapy, especially with respect to cancer. Increasingly, non-invasive MR temperature monitoring has been used as a tool for performance characterization of heating applicators and, more recently, to guide clinical thermal therapy treatments.<sup>1</sup> Recent investigations of rotating directional transurethral ultrasound applicators with MR temperature monitoring have demonstrated enhanced spatial control of heating distributions.<sup>2,3</sup> The objective of this study was to develop transurethral ultrasound applicators with axial and angular control of a heating distribution that do not require device manipulation during treatment. Rotating devices could impact the accuracy of the temperature measurement in the MR because the images are very sensitive to motion. The multi-sectored applicators developed in this study were able to conform a thermal dose to a target area within the prostate in a short time (~10min) under MR temperature monitoring.

**Methods** Transurethral ultrasound applicators, practical for treatment of the prostate (4mm OD delivery catheter, 10mm inflatable urethral cooling balloon), were constructed with 3.0mm OD and 6mm long sectored transducers. The tubular transducers (8-8.5MHz) were sectored into three 120° partitions by cutting a small notch in the outer electrode and part of the ceramic. Each transducer sector was powered individually at independent frequencies and power levels. A 2-D finite difference acoustic and biothermal model was used to evaluate the theoretical performance of the applicators. The model was based on the Pennes bioheat equation, incorporating dynamic changes in attenuation and perfusion as a function of temperature and thermal dose.

The heating distribution of the tri-sectored transurethral applicators was evaluated within three *in vivo* canine prostates in a 0.5T interventional scanner. A multiple channel radio frequency amplifier system was located directly outside the MR suite and supplied power to an applicator. Filters were used to reduce RF noise from the amplifier cables and prevent degradation of the MR images. MR temperature monitoring during the treatment was accomplished using the proton resonance frequency (PRF) shift method. The applied imaging parameters (TE/TR/flip/BW/FOV/slice = 21.4ms/150ms/60°/12.5kHz/20x12cm/5mm) allowed the temperature map to be updated about every 15s.<sup>4</sup> Multiple experiments were carried out with three slices monitored and displayed continuously, either along the length of the applicator (coronal) or orthogonal to the applicator (axial).

**Results** The *in vivo* experiments with multi-sectored transurethral ultrasound applicators displayed that the applicators could create continuous thermal lesions in a short amount of time (10min) and could be controlled with MR thermometry. Coronal MR temperature images of a tri-sectored transurethral applicator with two active sectors and two transducers are shown in Fig. 1. The applicator power levels were controlled to fit the 52°C (22°C increase) to boundary of the prostate using real-time visual inspection of the MR images. The white outline overlaid on the gross dissection slice of the prostate in Fig. 1(b) represents the imaging plane monitored in Fig. 1(a). A TTC stain that stains viable tissue red was performed following gross dissection immediately after the thermal treatment.

A biothermal simulation of a two-sectored heat from a tri-sectored applicator is also shown in Fig. 1(b). The simulation was done using a multi-point temperature controller fitted to an outlined treatment area from an MR image of a prostate with benign prostatic hyperplasia (BPH). The simulated results correlated very well with the two-sector *in vivo* prostate heat shown next to them.

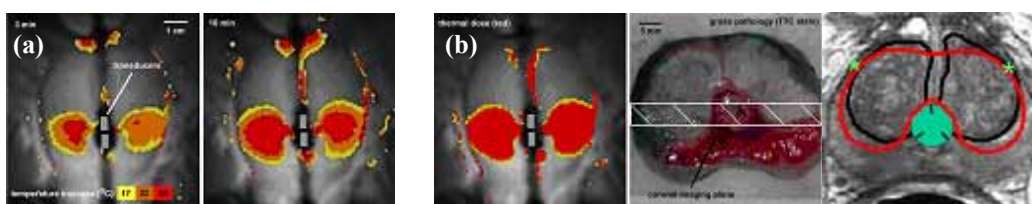


Figure 1. MR temperature images and thermal dose map of thermal lesion creation in canine prostate with a transurethral ultrasound applicator with 2 sectors active. Also, a biothermal simulation (red and black lines represent thermal dose and target area respectively) of a thermal treatment for BPH with a similar applicator.

**Summary** Transurethral ultrasound applicators for BPH and prostate cancer treatment with multiple sectors conformed a thermal dose to a simulated target area in the angular, axial, and radial dimensions. The applicators achieved radial penetration of at least 15mm and demonstrated axial and angular control with real-time MR temperature monitoring in three canine prostates. In conclusion, the multi-sectored ultrasound applicators developed in this study created large thermal lesions in relatively short treatment times (~10min). With real-time MR temperature imaging feedback, the devices were able deliver a targeted thermal dose without requiring any applicator movement or manipulation during treatment.

## References

1. Quesson B, *et al. J Magn Reson Imaging* **12**(4), 525 (2000).
2. Ross AB, *et al. Med Phys* **32**(6), 1555 (2005).
3. Chopra R, *et al. Phys Med Bio* **50**(21), 4957 (2005)
4. Butts Pauly, K, *et al. Proceedings Int Soc Therapeutic Ultrasound 2005*, Boston, MA (2005).

## Acknowledgements

The authors would like to recognize the generous gift from the Oxnard Foundation and NIH Grants CA88205, RR09784, CA77677, and CA111981 for supporting this work.